ACS OMEGA

http://pubs.acs.org/journal/acsodf

Article

LC-Q-TOF-MS Characterization of Polyphenols from White Bayberry Fruit and Its Antidiabetic Effect in KK-A^y Mice

Yilong Liu,[⊥] Xianan Zhang,[⊥] Liuhuan Zhan, Chang Xu, Linxiao Sun, Huamin Jiang, Chongde Sun, and Xian Li*

Cite This: *ACS Omega* 2020, 5, 17839−17849

Read Online

ACCESS | Metrics & More | Article Recommendations | Supporting Information

ABSTRACT: The present study is to investigate the polyphenolic composition and *in vivo* antidiabetic effect of white-fleshed Chinese bayberry cultivar "Shui Jing". By liquid chromatography quadrupole time-of-flight mass spectrometry (LC-Q-TOF-MS), 38 polyphenols were identified in the Shui Jing fruit extract (SJE), where proanthocyanidins (PAs), including epigallocatechin gallate (EGCG), as well as flavonols, including myricitrin and quercetrin, were the predominant ingredients. After a 5-week experiment, the SJE (200 mg/kg bodyweight) significantly reduced fasting blood glucose, elevated glucose tolerance, and insulin sensitivity in diabetic KK-A^y mice. It markedly attenuated bodyweight gain and decreased glycolipid metabolism-related markers including insulin, leptin, glucagon, triglyceride (TG), total cholesterol (TC), low-density lipoprotein cholesterol (LDL-c) and alanine aminotransferase (ALT) levels in mice. Liver weight and hepatic lipid accumulation were also significantly reduced by the SJE. Gene expressions of insulin 1 (*INS1*) and glycogen synthase kinase 3 β (*GSK3b*) were markedly inhibited while the hepatic phosphorylation of AMPKα was significantly increased in the liver of SJE-treated mice, indicating that the SJE may exert an antidiabetic effect through an AMPK-dependent pathway. In conclusion, white bayberry rich in PAs and flavonols may have great potential in the regulation of diabetes mellitus.

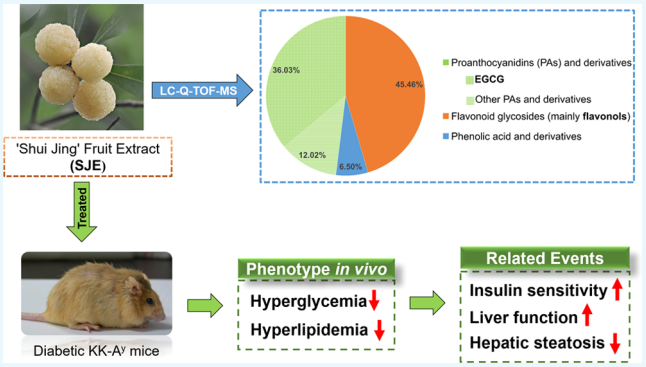

INTRODUCTION

Diabetes mellitus (DM) is a chronic disease resulting from the deficiency of insulin secretion (type-1 diabetes, T1D) or impairment of insulin action (type-2 diabetes, T2D), both of which result in hyperglycemia in the human body.[1] According to the World Health Organization (WHO), the global incidence of DM among adults over 18 years old have been steadily increasing over the past few decades.[2] In 2017, more than 451 million adults (age 18−99) were diagnosed with DM worldwide, and such a figure was estimated to reach 693 million by 2045.[3] T2D is the most prevalent diabetes accounting for more than 90% of all DM, and it is commonly associated with overweight and obesity,[2] and it could lead to severe life-threatening health complications, such as blindness, nephropathy, and cardiovascular disease.[4] Therefore, prevention and control programs are urgently needed to inhibit the dramatic rising incidence of T2D and its complications.

Plenty of epidemiological studies and meta-analysis showed that higher fresh fruit intake was associated with a significantly lower risk of T2D.[5,6] Moreover, substantial investigations indicated that fruit extracts from various dark-colored berries such as blueberry, mulberry, and blackberry possessed significant antidiabetic effects.[7,8] For example, in high fat diet-induced obese mice, blueberry supplement significantly elevated insulin sensitivity and glucose tolerance and showed protective effects on pancreatic β-cells.[9] Anthocyanin-rich blueberry consumption showed beneficial effects on glycemic control in T2D patients.[10] The mulberry anthocyanin extract regulated glucose metabolism through promoting glycogen synthesis and reducing gluconeogenesis in human HepG2 cells and markedly ameliorated insulin resistance (IR) in diabetic ob/ob mice.[11,12] As to blackberry, it showed a strong inhibitory effect on α-glucosidase that is linked to T2D and alleviated glycemia and IR in rats, demonstrating its potential benefit on the control or management of T2D.[13,14] All of these berries are rich in anthocyanins, which were known as the major functional ingredients due to their great antidiabetic potential.

Chinese bayberry (*Morella rubra* Sieb. et Zucc.), a dark-red colored berry native to China, is also a rich source of natural anthocyanins with cyanidin-3-*O*-glucoside (C3G) as the main component.[15,16] A series of research studies conducted by our

Received: June 11, 2020
Accepted: June 24, 2020
Published: July 8, 2020

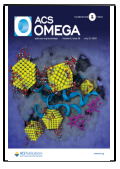

https://dx.doi.org/10.1021/acsomega.0c02759
ACS Omega 2020, 5, 17839−17849

group have shown that the C3G-rich bayberry extract had significant anti-hyperglycemic effects *in vivo* and *in vitro*.[17−21] The bayberry fruit extract achieved remarkable enhancement of glucose consumption in a concentration-dependent manner in HepG2 cells.[17] Furthermore, the C3G-rich components showed protective effects on isolated islets from mice or neonatal pigs and enhanced their function after transplantation.[18,19] the C3G-rich bayberry pulp extract ameliorated hyperglycemia in streptozotocin (STZ)-induced diabetic mice,[20] markedly lowered the fasting blood glucose levels, and improved the glucose tolerance and insulin sensitivity in diabetic KK-A^{y} mice.[21] These results demonstrated that red Chinese bayberry showed excellent antidiabetic properties in which C3G plays an important role. Interestingly, there is a special white bayberry cultivar, namely "Shui Jing" (Figure 1A), which differs from the common red or dark-red cultivars, with a low content of anthocyanins.[16] So far, no study was performed on the antidiabetic activity of white bayberry fruits, which attracted our great interest.

Hence, the present study was designed to characterize and quantify polyphenolic compounds of the Shui Jing fruit extract (SJE) by liquid chromatography quadrupole time-of-flight mass spectrometry (LC-Q-TOF-MS) and evaluate its antidiabetic effect *in vivo* using KK-A^{y} mice as an experimental model. Possible mechanisms of its anti-hyperglycemic effects were also investigated and discussed.

RESULTS

Qualitative and Quantitative Analysis of Polyphenols in the SJE. The SJE was characterized by LC-Q-TOF-MS for polyphenolic profiles. Compound identification was performed according to mass spectrometry data under negative ESI mode, published literature data, and comparison with an authentic standard, wherever available. Eventually, a total of fifteen phenolic acids and derivatives, nine flavonoid glycosides, and 14 proanthocyanidins (PAs) and derivatives were identified. Combined with the quantitative analysis of polyphenols in the SJE, the main ingredients accounting for 90.80% of total polyphenols are listed in Table 1 and other polyphenolic compounds at a relatively lower level are listed in Table S1.

In the SJE, PAs and derivatives (48.05%) were the most representative class (Figure 1C). Particularly, compound **1** showed the largest amount of 1706.09 ± 16.87 mg/100 g DW (Table 1) that accounted for 36.03% of the total polyphenolic content. It showed a deprotonated molecular ion $[M - H]^-$ at m/z 457. The base peak at m/z 169 (relative abundance (RA) 100%) corresponds to gallic acid and that at m/z 305 corresponds to the (E)GC unit. Fragment ion at m/z 125 could be attributed to the loss of −COO (44 Da) from m/z 169, which confirmed that it contained the gallic acid group. Based on the comparison with literature data and authentic standard confirmation, compound **1** was identified as epigallocatechin gallate (EGCG). Compound **3** produced a parent ion at 305, and the major fragment ion at m/z 125 (RA 100%) corresponds to a trihydroxybenzene moiety. It was confirmed by matching retention time and MS^{n} spectral data with a chemical standard of EGC. In addition, some polymers related to (E)GC or (E)GCG such as (E)GC-(E)GCG (compounds **2**) and (E)GCG-(E)GCG (compound **4**) were also identified as the major PAs in the SJE (Table 1).

Flavonoid glycosides (45.46%) were another major class found in the SJE (Figure 1C), with myricitrin (compound **5**, 834.18 ± 4.51 mg/100 g DW) as the principal component

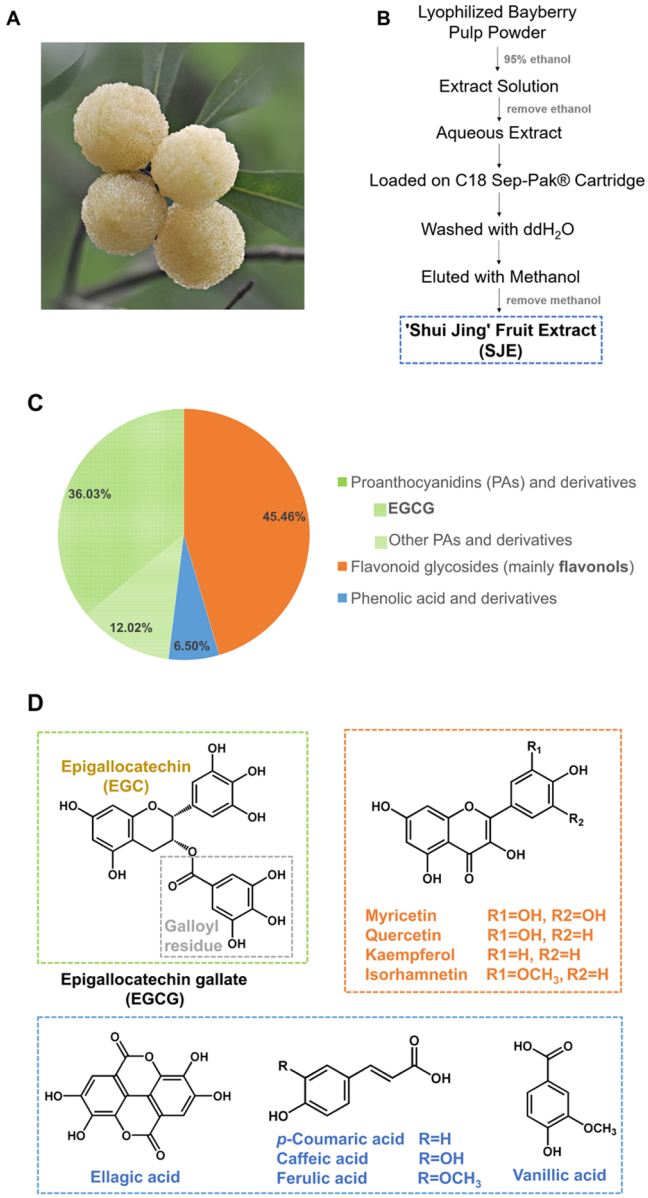

Figure 1. (A) Shui Jing cultivar of the Chinese bayberry fruit. (B) Schematic diagram for the preparation of the Shui Jing fruit extract (SJE). (C) Pi chart representation of the polyphenolic composition in the SJE. (D) Aglycons of the proanthocyanidins (PAs) and derivatives, flavonoid glycosides, and phenolic acid and derivatives.

followed by quercetrin (779.95 ± 4.31 mg/100 g DW) (Table 1). Myricitrin and compound **9** were identified based on literature information and further confirmation by matching retention time and MS^{n} spectral data with authentic standards. Compound **6** showed an $[M - H]^-$ ion at 447. Base peaks at m/z 300 $[M - 2H - 146]^-$ (RA 100%) and 301 $[M - H - 146]^-$ (RA 61%) confirmed the quercetin aglycon after cleavage of a rhamnosyl residue (146 Da). Hence, it was identified as quercetrin. Compound **7** showed a deprotonated molecular ion at m/z 431 corresponding to the molecular formula, $C_{21}H_{20}O_{10}$, of sugar-substituted flavonols. Further fragmentation by collision-induced dissociation of this parent ion (m/z 431) gave aglycon fragments (kaempferol) at m/z 285 $[M - H - 146]^-$ (RA 100%) and 284 $[M - 2H - 146]^-$ (RA 81%) after the loss of a rhamnosyl residue. Combined with the literature data, compound **7** was identified as

https://dx.doi.org/10.1021/acsomega.0c02759
ACS Omega 2020, 5, 17839−17849

Table 1. Main Polyphenols Identified by Liquid Chromatography Quadrupole Time-of-Flight Tandem Mass Spectrometry (LC-Q-TOF-MS) and Their Contents in the Shui Jing Fruit Extract (SJE)

no.	compound	RT[a] (min)	$[M-H]^-$ (m/z)	molecular formula	fragment ions (relative abundance)	refs	content (mg/100 g DW)
				Proanthocyanidins and Derivatives			
1	[b]EGCG[d]	32.891	457.0775	$C_{22}H_{18}O_{11}$	305.0671(14), 169.0143(100), 125.0247(37.5)	22	1706.09 ± 16.87
2	(E)GC-(E)GCG	23.483	761.1366	$C_{37}H_{30}O_{18}$	609.1294(19), 591.1182(18), 423.0739(100), 305.0675(29)	23	185.37 ± 2.74
3	[c]EGC[d]	21.168	305.0669	$C_{15}H_{14}O_7$	125.0243(100), 219.0654(30), 221.0451(15), 165.0197(25)	24	127.44 ± 0.67
4	(E)GCG-(E)GCG	30.964	913.1485	$C_{44}H_{34}O_{22}$	761.144(36), 743.133(33), 591.1191(42), 573.1077(23), 423.0738(100), 285.0407(23)	25	98.58 ± 1.00
				Flavonoid Glycosides			
5	myricetin-3-*O*-α-L-rhamnoside (myricitrin)[d]	44.885	463.0876	$C_{21}H_{20}O_{12}$	317.0309(29), 316.0221(100), 287.0193(26), 271.0243(35), 259.0244(7)	17	834.18 ± 4.51
6	quercetin-3-*O*-rhamnoside (quercetrin)	53.954	447.093	$C_{21}H_{20}O_{11}$	301.0349(61), 300.0271(100), 271.0247(48), 255.03(30), 243.0298(11), 151.0033(7)	26	779.95 ± 4.31
7	kaempferol-3-*O*-rhamnoside	62.243	431.0981	$C_{21}H_{20}O_{10}$	285.0409(100), 284.033(81), 255.0304(75), 227.0352(40), 229.0508(13)	27	279.14 ± 1.79
8	myricetin-3-*O*-(2″-*O*-galloyl)-α-L-rhamnopyranoside	61.781	615.0991	$C_{28}H_{24}O_{16}$	463.0918(9), 317.0309(100), 178.9984(9)	28	118.41 ± 1.35
9	cyanidin-3-*O*-glucoside[d]	18.304	449.1078	$C_{21}H_{20}O_{11}$	284.0324(100), 447.0954(74)	17	78.52 ± 0.16
				Phenolic Acid and Derivatives			
10	3′-*O*-methyl-4-*O*-(β-D-xylopyranosyl) ellagic acid	52.823	447.0576	$C_{20}H_{16}O_{12}$	315.0153(100), 299.9921(96), 285.0401(7), 284.0329(21), 255.0293(12), 227.034(12)	29	92.31 ± 0.04

[a]RT: Retention time. [b]EGCG: Epigallocatechin gallate. [c]EGC: Epigallocatechin. [d]Further confirmed in comparison with authentic standard and its quantitative analysis was absolute. Others were relatively quantified.

kaempferol-3-*O*-rhamnoside. Compound **8** gave precursor ion $[M-H]^-$ at m/z 615 ($C_{28}H_{24}O_{16}$). It generated a product ion at m/z 463 $[M-H-152]^-$ by loss of a galloyl moiety. Another ion at m/z 317 $[M-H-152-146]^-$ (RA 100%) was corresponding to cleavage of galloyl and a deoxyhexose moiety. Based on a comparison with a reported compound, this compound was confirmed as myricetin-3-*O*-(2″-*O*-galloyl)-α-L-rhamnopyranoside.

Phenolic acid and derivatives were also identified but at a relatively lower percentage (Figure 1C), where compound **10** was the predominant ingredient. It showed the parent ion at m/z 447 ($C_{20}H_{16}O_{12}$). The base peaks at m/z 315 $[M-H-132$ Da (xylopyranose unit)$]^-$ (100% RA) and 300 (96% RA) were predominant. Such characterization was the same as a previous report. Thus, this peak was identified as 3′-*O*-methyl-4-*O*-(β-D-xylopyranosyl) ellagic acid. Chemical structures of aglycons in each class are presented in Figure 1D.

Bodyweight, Food Intake, and Tissue Index. As shown in Table 2, compared with nondiabetic C57BL/6 mice, diabetic KK-A^y mice showed obesity and bodyweight (BW) was steadily increasing during the 5 week experiment. However, such an increasing trend was attenuated in the SJE group. From week 2 to 5, the bodyweight (BW) of KK-A^y mice supplemented with the SJE was markedly lower than that of the KK-A^y control group ($p < 0.05$ or $p < 0.01$) (Table 2). With regard to food intake, no remarkable difference was observed between two groups of KK-A^y mice. The weight of adipose tissues, *i.e.*, epididymal and perirenal white adipose tissue (WAT) and dorsal brown adipose tissue (BAT), in heart and kidneys showed no difference between the SJE and its control group (Table 2). While the liver index of the SJE group (3.88 ± 0.18%) was significantly lower than the KK-A^y control group (5.11 ± 0.29%) ($p < 0.05$) and even close to that of the nondiabetic C57BL/6 group (3.79 ± 0.24%) (Table 2).

Fasting Blood Glucose (FBG), Oral Glucose Tolerance Test (OGTT), and Insulin Tolerance Test (ITT). As for FBG, C57BL/6 mice showed normal levels, while diabetic KK-A^y mice showed hyperglycemic symptoms during the experiment (Figure 2A). At the beginning of the study, there was no significant difference in the initial FBG levels between two groups of diabetic mice. The FBG concentration of the KK-A^y control group increasingly rose up during the 5 week experiment and eventually reached a maximum of 23.58 ± 2.70 mmol/L (Figure 2A). Notably, the SJE supplement significantly inhibited such an increase in the FBG level since week 2 ($p < 0.01$ or $p < 0.001$) (Figure 2A). Finally, the blood glucose level of the SJE group (9.96 ± 1.16 mmol/L) achieved a nearly 50% decrease compared with that of the KK-A^y control group (23.58 ± 2.70 mmol/L) ($p < 0.001$) (Figure 2A).

OGTT was performed on week 4. In the KK-A^y control group, blood glucose levels were still high with a concentration of 22.52 ± 2.90 mmol/L at 1 h and 20.33 ± 2.75 mmol/L at 2 h after gavage with glucose, indicating an apparently impaired glucose tolerance (Figure 2B). Supplement of the SJE elevated the glucose tolerance in KK-A^y mice, where blood glucose concentrations reduced to 13.34 ± 2.01 mmol/L at 1 h and 10.24 ± 1.62 mmol/L at 2 h after oral glucose (Figure 2B). In addition, diabetic mice administered with the SJE showed markedly lower blood glucose levels compared to the corresponding control mice at each time point in the OGTT ($p < 0.01$ or $p < 0.001$) (Figure 2B). Such results indicated that the SJE had a high regulation activity on glucose tolerance in diabetic mice.

ITT was conducted on week 5 to test the effect of SJE supplement on insulin sensitivity. Insulin exerted a stronger glucose-lowering effect in the SJE group mice than that in the water-treated control group (Figure 2C). Moreover, blood glucose levels in SJE-treated mice showed significant differences at each time point in ITT ($p < 0.001$), compared with water-treated KK-A^y mice (Figure 2C). These results

https://dx.doi.org/10.1021/acsomega.0c02759
ACS Omega 2020, 5, 17839−17849

Table 2. Effects of the SJE[a] (200 mg/kg Bodyweight (BW)) on Growth Parameters, Tissue Index, and Serum Parameters in Diabetic KK-A^y Mice

parameters	C57BL/6 + water[b]	KK-A^y + water[c]	KK-A^y + SJE[c]
Bodyweight (g)			
0 week	22.24 ± 0.72	36.89 ± 0.68	37.05 ± 0.61
1 week	25.04 ± 0.86	39.57 ± 0.75	38.75 ± 0.47
2 week	25.78 ± 0.81	41.76 ± 1.05	38.77 ± 0.53*
3 week	26.24 ± 1.05	43.57 ± 1.05	39.41 ± 0.77**
4 week	26.88 ± 1.04	45.75 ± 1.19	40.73 ± 0.53**
5 week	24.32 ± 0.77	46.76 ± 1.56	41.82 ± 0.65*
food intake (g per day)	2.99 ± 0.09	5.29 ± 0.05	5.01 ± 0.08
Tissue Index (%)[d]			
liver	3.79 ± 0.24	5.11 ± 0.29	3.88 ± 0.18*
epididymal WAT[e]	1.00 ± 0.19	2.63 ± 0.13	2.44 ± 0.09
perirenal WAT	0.19 ± 0.07	1.29 ± 0.11	1.08 ± 0.07
BAT[f]	0.31 ± 0.05	0.63 ± 0.07	0.87 ± 0.15
heart	0.53 ± 0.06	0.34 ± 0.01	0.37 ± 0.01
kidney	1.13 ± 0.09	0.99 ± 0.03	1.00 ± 0.02
Serum Lipids			
TC[g] (mmol/L)	2.13 ± 0.24	3.77 ± 0.32	2.70 ± 0.13*
TG[h] (mmol/L)	0.64 ± 0.06	0.74 ± 0.02	0.60 ± 0.02*
HDL-c[i] (mmol/L)	2.18 ± 0.16	1.72 ± 0.19	2.34 ± 0.11*
LDL-c[j] (mmol/L)	0.05 ± 0.02	0.53 ± 0.11	0.19 ± 0.04*
Liver Function			
ALT[k] (U/L)	27.5 ± 1.06	66.71 ± 10.79	38.25 ± 3.75*
AST[l] (U/L)	112.5 ± 7.85	138.86 ± 9.96	122.75 ± 8.34
AST/ALT	4.11 ± 0.31	2.28 ± 0.16	3.36 ± 0.28**

[a]SJE: Shui Jing fruit extract. [b]C57BL/6 mice as nondiabetic control (n = 10). [c]KK-A^y mice as a diabetic model (n = 10 for each group). [d]Tissue index (%) = tissue weight (g)/bodyweight (g) × 100. [e]WAT: White adipose tissue. [f]BAT: Brown adipose tissue. [g]TC: Total cholesterol. [h]TG: Triglycerides. [i]HDL-c: High-density lipoprotein cholesterol. [j]LDL-c: Low-density lipoprotein cholesterol. [k]ALT: Alanine aminotransferase. [l]AST: Aspartate transaminase. Values are expressed as the mean ± standard error (SE). *p < 0.05, **p < 0.01, compared to the KK-A^y + water group.

demonstrated that the SJE might improve IR and increase the efficiency of insulin action.

Serum Analysis. After the 5 week experiment, serum triglyceride (TG), total cholesterol (TC), low-density lipoprotein cholesterol (LDL-c), and alanine aminotransferase (ALT) concentrations were significantly decreased, and the high-density lipoprotein cholesterol (HDL-c) level was markedly increased in the SJE group mice, compared to that in KK-A^y control mice (p < 0.05) (Table 2). The SJE-treated mice also showed remarkably lower levels in serum insulin (29.73 ± 1.56 *vs* 17.3 ± 3.38 mU/L, p < 0.05), glucagon (168.71 ± 7.55 *vs* 138.36 ± 7.88 pg/mL, p < 0.05), and leptin (4.35 ± 0.19 *vs* 3.09 ± 0.15 ng/mL, p < 0.001) than that in control group (Figure 3). Serum resistin and adiponectin levels tended to be decreased in the SJE group mice compared with the control group (Figure 3).

Hepatic Lipid Parameters and Histological Observation. To study the effects of the SJE on hepatic lipid abnormalities, TC and TG concentrations in mice liver were detected and histological analysis was conducted (Figure 4). The results showed that the liver weight of SJE-treated KK-A^y mice was significantly decreased compared to the control

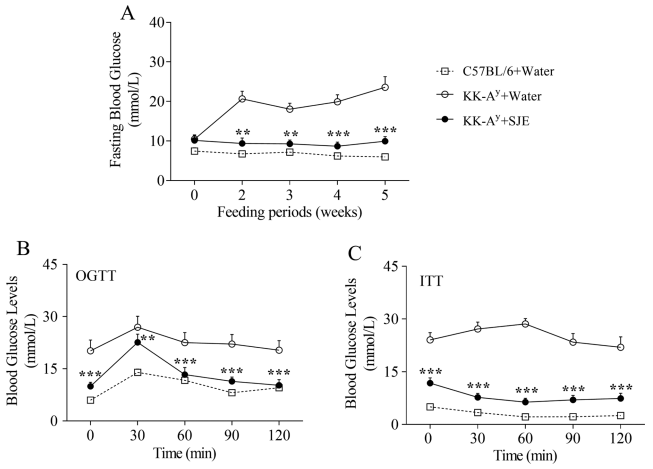

Figure 2. Effects of the SJE at a dose of 200 mg/kg BW on fasting blood glucose (A), oral glucose tolerance (B), and insulin resistance (C) in diabetic KK-A^y mice during the 5 week experiment, with an oral glucose tolerance test (OGTT) in week 4 and the insulin tolerance test (ITT) in week 5. Values are mean ± SE of 7−10 mice. *p < 0.05, **p < 0.01, and ***p < 0.001; the KK-A^y + SJE group compared to the KK-A^y + water group.

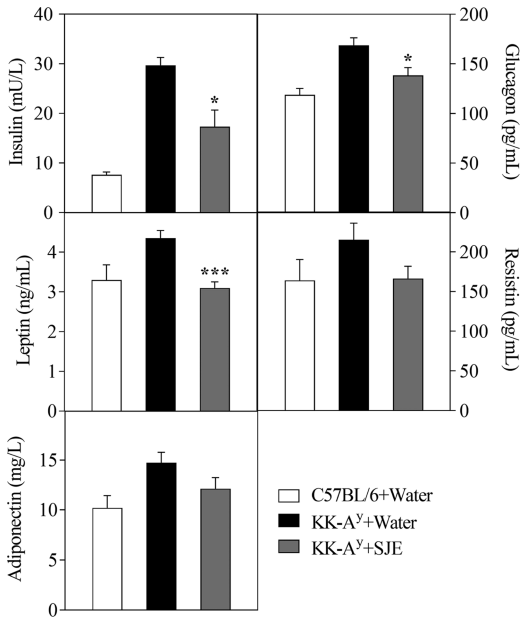

Figure 3. Effects of the SJE at a dose of 200 mg/kg BW on levels of serum insulin, glucagon, leptin, resistin, and adiponectin in diabetic KK-A^y mice at the end of the experiment. Values are expressed as mean ± SE (n = 7−10). *p < 0.05 and ***p < 0.001; the KK-A^y + SJE group compared to the KK-A^y + water group.

group (p < 0.05). Both hepatic TC and TG levels in diabetic mice were markedly reduced by the SJE (p < 0.01) (Figure 4A). According to the histological observation by either hematoxylin and eosin (H&E) staining or Oil Red O staining on the liver of diabetic KK-A^y control mice, the shapes of hepatocytes become irregular, as severe fatty infiltration was shown in liver tissues and lipid droplets were intensely accumulated in hepatocytes (Figure 4B). As expected, SJE administration significantly inhibited lipid droplet accumulation in hepatocytes and alleviated hepatic steatosis (Figure 4B).

https://dx.doi.org/10.1021/acsomega.0c02759
ACS Omega 2020, 5, 17839−17849

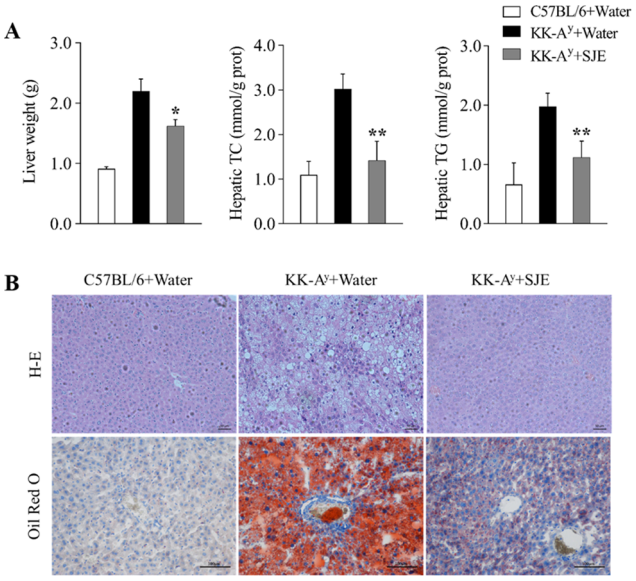

Figure 4. (A) Liver weight, hepatic cholesterol (TC) level, and hepatic triglyceride level (TG) in diabetic KK-A^y mice (n = 5); (B) Hematoxylin and eosin staining and Oil Red O staining of transverse liver section (200× magnification) (n = 5). Values are expressed as mean ± SE. *p < 0.05 and **p < 0.01; the KK-A^y + SJE group compared to the KK-A^y + water group.

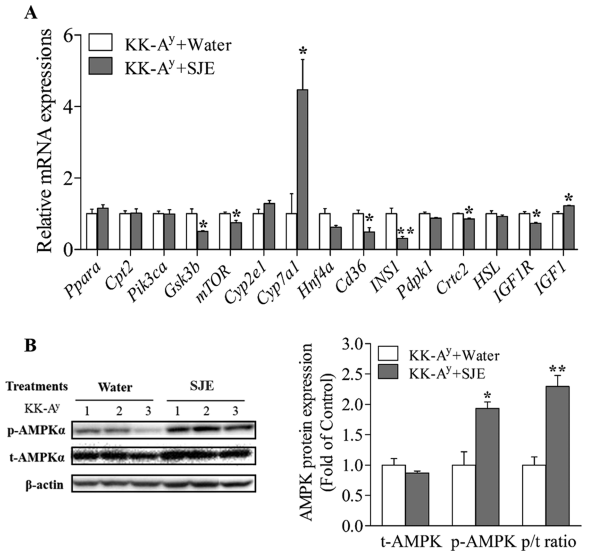

Figure 5. (A) Gene expressions of hepatic glucose and lipid metabolism markers related to the AMPK pathway in the liver of diabetic KK-A^y mice (n = 3). (B) Effects of the SJE (200 mg/kg BW) on p-AMPKα protein expression in the liver of diabetic KK-A^y mice (n = 3). Values are expressed as mean ± SE. *p < 0.05 and **p < 0.01; the KK-A^y + SJE group compared to the KK-A^y + water group.

Gene and Protein Expression Analysis. To explore the possible mechanism of hepatic glucose and lipid homeostasis regulation by the SJE, the mRNA levels of fifteen genes (Table 3) were analyzed by real-time polymerase chain reaction (PCR) in the liver of KK-A^y diabetic mice (Figure 5A).

The results showed that gene expressions of glycogen synthase kinase 3 β (*Gsk3b*), the mammalian target of rapamycin (*mTOR*), the cluster of differentiation 36 (*Cd36*), insulin 1 (*INS1*), CRE-binding protein (CREB)-regulated transcription coactivator 2 (*Crtc2*), and the insulin-like growth factor 1 receptor (*IGF1R*) were significantly decreased by the SJE treatment (Figure 5A). Additionally, gene expressions of cholesterol 7alpha-monooxygenase (*Cyp7a1*) and insulin-like growth factor 1 (*IGF1*) were markedly upregulated in the liver of the SJE-treated group compared to the control group (Figure 5A). These glycolipid metabolism-related genes that are markedly regulated by the SJE were all involved in the AMPK pathway.

Phosphorylation of AMPKα, which is required for AMPK activation, was also examined by western blot (Figure 5B). The results showed that the SJE treatment significantly elevated the phosphorylation of AMPKα and the ratio of phosphorylated to total AMPKα in mice liver compared to that in the KK-A^y

Table 3. Primer Sequences Used for qPCR in This Study[a]

genes	forward (5′ to 3′)	reverse (5′ to 3′)
Ppara	AGAGCCCCATCTGTCCTCTC	ACTGGTAGTCTGCAAAACCAAA
Cpt2	CAGCACAGCATCGTACCCA	TCCCAATGCCGTTCTCAAAAT
Pik3ca	TTATTGAACCAGTAGGCAACCG	GCTATGAGGCGAGTTGAGATCC
Gsk3b	TGGCAGCAAGGTAACCACAG	CGGTTCTTAAATCGCTTGTCCTG
mTOR	ACCGGCACACATTTGAAGAAG	CTCGTTGAGGATCAGCAAGG
Cyp2e1	GGACCTTTCCCAATTCCTTTCTT	TCTTGTGGTTCAGTAGCACCT
Cyp7a1	GGGATTGCTGTGGTAGTGAGC	GGTATGGAATCAACCCGTTGTC
Hnf4a	AAGGTGCCAACCTCAATTCATC	CACATTGTCGGCTAAACCTGC
Cd36	ATGGGCTGTGATCGGAACTG	TTTGCCACGTCATCTGGGTTT
INS1	CACTTCCTACCCCTGCTGG	ACCACAAAGATGCTGTTTGACA
Pdpk1	CTGTATGACGCTGTGCCCATT	AAGGGGTTGGTGCTTGGTC
Crtc2	ACAGCCTCAGCGTCCAATC	GTGGAGCCGATGTCCATCAT
HSL	CCAGCCTGAGGGCTTACTG	CTCCATTGACTGTGACATCTCG
IGF1R	CATGTGCTGGCAGTATAACCC	TCGGGAGGCTTGTTCTCCT
IGF1	CTGGACCAGAGACCCTTTGC	GGACGGGGACTTCTGAGTCTT
β-actin	GGCTGTATTCCCCTCCATCG	CCAGTTGGTAACAATGCCATGT

[a]*Ppara*, peroxisome proliferator-activated receptor α. *Cpt2*, carnitine O-palmitoyltransferase 2. *Pik3ca*, phosphatidylinositol-4,5-bisphosphate 3-kinase catalytic subunit α. *Gsk3b*, glycogen synthase kinase 3 β. *mTOR*, mammalian target of rapamycin. *Cyp2e1*, cytochrome P450, family 2, subfamily E, polypeptide 1. *Cyp7a1*, cholesterol 7alpha-monooxygenase. *Hnf4a*, hepatocyte nuclear factor 4-α. *CD36*, cluster of differentiation 36. *INS1*, insulin 1. *Pdpk1*, 3-phosphoinositide dependent protein kinase-1. *Crtc2*, CRE-binding protein (CREB)-regulated transcription coactivator 2. *HSL*, hormone-sensitive lipase. *IGF1*, insulin-like growth factor 1. *IGF1R*, insulin-like growth factor 1 receptor.

https://dx.doi.org/10.1021/acsomega.0c02759
ACS Omega 2020, 5, 17839−17849

control group (Figure 5B). Overall, the SJE may exert the antidiabetic effect through an AMPK-dependent pathway.

DISCUSSION

Anthocyanin in colored berries is known as the most abundant polyphenol possessing significant anti-hyperglycemic potential.[8] However, the antidiabetic effect of non-anthocyanin components in berry fruits draws much less attention. In the present study, KK-A^y mouse, which phenotypically resembles human T2D, was selected as an animal model for the *in vivo* antidiabetic study on the SJE. The results showed that the hyperglycemia symptom of diabetic KK-A^y mice was significantly attenuated in the SJE-treated group, where it markedly reduced fasting glucose during the 5 week experiment. At the end of the experiment, the FBG level of the SJE group was greatly reduced compared with that of the KK-A^y control mice (9.96 ± 1.16 *vs* 23.58 ± 2.70 mmol/L). In our previous study, the FBG level was also significantly reduced in KK-A^y mice treated with the red Chinese bayberry extract that is rich in anthocyanins.[21] These results proved that white berry fruits accumulating low amounts of anthocyanins also had excellent glucose-lowering properties. It was reported that white grape extracts had potent inhibitory activity on α-amylase and α-glucosidase,[30] and white grape wine significantly ameliorated oxidative stress in STZ-induced diabetic rats.[31]

To identify the main ingredients contributing to its antidiabetic activity, the phytochemical characterization of SJE was performed. PAs were the main phenolic compounds in the SJE, and EGCG was identified as the most abundant component. EGCG is known as a predominantly active compound in green tea that has been found to possess a number of biological activities for the prevention or treatment of DM, obesity, *etc*.[32,33] PAs such as EGCG are strong antioxidants, and the antioxidant activity plays an important role in reducing the insulin insensitivity or protecting the β cells from oxidative stress caused by various factors.[34,35] Our previous reports showed that the litchi fruit extract rich in PAs significantly increased the glucose consumption in HepG2 cells, and such bioactivity was highly linked to the antioxidant capacity and total PA content of different cultivars.[36,37]

As far as the flavonoid glycosides in the SJE, flavonols including myricitrin and quercetrin were the main components, and both of which were reported to show significant inhibitory effects on α-glucosidase, an important target for the treatment of T2D with impaired glucose tolerance.[38] Our previous report showed that quercetrin remarkably increased the glucose consumption in HepG2 cells.[17] As to myricitrin, it markedly relieved oxidative damage induced by the hyperglycemic condition in C2C12 cells and exhibited the *in vivo* antidiabetic effect by recovering body and tissue weight, improving antioxidant stress and hyperglycemia on STZ-nicotinamide-induced diabetic mice.[39,40] Here, the SJE rich in myricitrin and quercitrin improved the glucose tolerance in KK-A^y mice. C3G was also identified in the SJE with a content of 78.52 ± 0.16 mg/100 g DW, which was much lower than that of the red-fleshed bayberry extract ranging from 7623 to 42 093 mg/100 g DW.[17]

IR is an important hallmark in the occurrence and development of T2D, and insulin secretion is promoted to maintain glucose homeostasis.[41] Leptin is also important for glucose homeostasis regulation, which can reduce serum glucose and insulin concentrations in ob/ob mice.[42] In this study, KK-A^y mice showed phenotypes of hyperinsulinemia and hyperleptinemia, indicating that it developed IR and leptin resistance. Interestingly, the SJE administration improved such symptoms in diabetic KK-A^y mice as shown in significantly reduced serum insulin and leptin and elevated insulin sensitivity in ITT. Glucagon is a hormone stimulating gluconeogenesis and glycogenolysis, leading to increased production of hepatic glucose, which was mobilized to maintain normoglycemia in the fasting state.[43] It exhibits an antagonist effect against insulin and shows abnormally elevated levels in the blood circulation of T2D patients.[44] In our study, the hyperglucagonemia symptom in KK-A^y mice was alleviated by SJE treatment accompanied by a significantly lowered serum glucagon concentration.

Increased hepatic glucose output via elevated gluconeogenesis is the main cause of fasting hyperglycemia in individuals with T2D.[45,46] In the present study, *GSK3b* and *Crtc2* mRNA levels were markedly decreased in SJE-treated KK-A^y mice liver compared with that in control mice ($p < 0.05$). GSK3b is a crucial enzyme of glycogen synthesis, which is involved in blood glucose regulation, insulin deficiency, and IR.[47] It acts as a negatively regulated substrate of the insulin signaling pathway that, when genetically reduced, improves glucose homeostasis in an insulin-resistant mouse.[48] Hence, modulation of hepatic GSK3b activity may be of benefit for systemic glucose homeostasis. EGCG was capable of enhancing glycogen synthesis by promotion of GSK3b phosphorylation and inhibiting lipogenesis in hepatocytes, which was associated with elevated expression of phosphorylated AMPK.[49] Phenolic acids, which were also observed in the SJE at relatively lower levels, were reported to have significant antidiabetic activities by increasing glucose uptake and glycogen synthesis, thus improving glucose profiles in DM.[50] Crtc2 plays a pivotal role in the gluconeogenic program as a critical downstream target of AMPK.[46,51] As reported, AMPK is a key player in maintaining glucose homeostasis, which is placed at the center stage in the study of DM.[52] In our study, SJE significantly activated AMPK in diabetic KK-A^y mice liver, indicating that the SJE may inhibit the hepatic glucose output through activating AMPK, blocking *Crct2* in liver gluconeogenesis to relief fasting hyperglycemia. Similarly, metformin, a widely used oral drug for the treatment of T2D, also works by activating AMPK and blocking hepatic gluconeogenesis.[53,54]

mTOR that functions as serine/threonine protein kinase is dysregulated in many human diseases including T2D and obesity.[55] The mTOR pathway is activated during multiple cellular processes such as IR and adipogenesis[55] and is one of the major downstream signaling pathways regulated by AMPK.[56] It integrates the input from upstream pathways, including insulin and growth factors (*e.g.*, IGF1).[57] IGF1 is a hormone that shared a similar molecular structure to insulin and is produced primarily by the liver.[58] It exerts glucose-regulation actions by binding to IGF1R.[59] Marked down-regulation on gene expressions of *mTOR*, *IGF1*, and *IGF1R* was observed in SJE-treated mice compared with the control group, indicating that the SJE might attenuate IR in the diabetic mice by at least partly modulation on the mTOR pathway. Additionally, a downstream gene in the mTOR pathway, *CD36*, which is involved in lipogenesis,[60] was markedly downregulated in the liver of SJE-treated mice compared to that of water-treated control mice. Meanwhile, the mRNA levels of *Cyp7a1* involved in cholesterol metabolism were markedly increased by the SJE, exhibiting the same function as C3G.[61] Combined with the significantly

https://dx.doi.org/10.1021/acsomega.0c02759
ACS Omega 2020, 5, 17839−17849

reduced TG and TC levels, as well as the number and size of hepatic lipid droplets, it seems that the coordinated action of improvement in hepatic adipogenesis and cholesterol regulation contributed to the alleviation effect of the SJE on hepatic steatosis in diabetic KK-A^y mice. In accord with our results, EGCG supplements exerted significant anti-hyperglycemic and anti-dyslipidemia activities in STZ-nicotinamide-induced T2D diabetic rats as shown in the remarkably reduced plasma glucose levels and lipid profiles such as TG, TC, and LDL-c.[62]

In conclusion, the present study characterized and quantified polyphenolic profiles in the SJE, where PAs and derivatives such as EGCG, as well as flavonols such as quercetrin and myricitrin were the main ingredients. The SJE rich in such polyphenols exerted significantly anti-hyperglycemic properties through an AMPK-dependent pathway. Therefore, white bayberry is also an excellent natural antidiabetic food, which may suggest its potential application as a functional food ingredient or for further drug discovery in the prevention and control of DM and its complications.

MATERIALS AND METHODS

Chemicals. Standards of ellagic acid (≥96%), *p*-coumaric acid (≥99%), quercetin-3-*O*-glucoside (isoquercetrin) (≥98%), C3G (≥98%), myricetin-3-*O*-*α*-L-rhamnoside (myricitrin) (≥98%), EGCG, and EGC (≥98%) were purchased from Aladdin (Shanghai, China). Methanol and acetonitrile for liquid chromatography were of chromatographic grade, and all of the other solvents used in the experiment were of analytical grade from Sinopharm Chemical Reagent Co., Ltd. (Shanghai, China).

Preparation of the SJE. Shui Jing fruits were harvested at commercial maturity from Xianju county, Zhejiang province, China. The pulp was lyophilized and ground into powder in a laboratory mill. The SJE was prepared according to our previous publication with minor modifications,[17] and the schematic diagram of its preparation is shown in Figure 1B. Lyophilized bayberry pulp powder was extracted twice with 95% aqueous ethanol containing 1% formic acid, as the solid-to-liquid ratio of 1:40. It was stirred well and sonicated for 30 min. The ultrasonic power and frequency were 30 W and 60 kHz, respectively. Then, the extract was centrifuged at 10 000 rpm for 10 min to obtain the supernatants. Combined supernatants were evaporated under reduced pressure with a rotary evaporator to remove ethanol. The remaining aqueous extract solution was then loaded on a C18 Sep-Pak cartridge (12 cc/2 g, waters) after activating the cartridge with 20 mL of methanol and conditioning with 20 mL of ddH_2O. The cartridge was then washed with ddH_2O to remove impurities such as sugars and eluted with methanol to get the eluents, which were vacuum-dried (Concentrator Plus, Eppendorf, Germany) to obtain the SJE for further analysis.

Characterization and Quantification of Polyphenols in the SJE. *Identification of Polyphenols by LC-Q-TOF-MS.* Phytochemical characterization of the SJE was conducted using a quadrupole time-of-flight mass spectrometer (AB Triple TOF 5600plus System, AB SCIEX, Framingham, MA), which was coupled with an ultraperformance liquid chromatography system (ACQUITY UPLC, Waters Corp., Milford, MA).[16] Chromatographic separation was achieved using an ODS C18 analytical column (4.6 mm × 250 mm, Waters Corp.). The column was kept at 25 °C, and the flow rate was 1 mL/min. The mobile phase solutions were water with 0.1% formic acid (eluent A) and acetonitrile: 0.1% formic acid (1:1, v/v) (eluent B) and were implemented in the following gradient: 0−40 min, 10−38% B; 40−60 min, 38−48% B; 60−70 min, 48−100% B; 70−75 min, 100−10% B; and 75−80 min, 10% B. All samples were kept at 4 °C during the analysis. The injection volume was 5 μL.

MS conditions were as follows: the scan range was set at m/z 100−2000. The source voltage was −4.5 kV in negative mode, and the temperature was 550 °C. The pressure of gases 1 and 2 was set to 60 psi. Curtain gas (N_2) was set to 35 psi. The MS/MS fragmentation process was accomplished at collision energies of −20, −40, and −60 eV in IDA data acquisition mode. The maximum allowed error was set to ±5 ppm. AB Sciex Analyst Software Package Version 1.6 was applied to control the entire system and data acquisition. Peakview2.2 Software was used for data processing.

The identification of phytochemicals was performed based on the accurate mass and mass spectrometric fragmentation patterns guided by the Massbank of North America database (MoNA, https://mona.fiehnlab.ucdavis.edu), the ChemSpider database (http://www.chemspider.com/), the published literature, and commercial standards and theoretical MS/MS tags.

Quantification of Polyphenols in Multiple Reaction Monitoring (MRM) Mode by LC-MS. For quantification of phytochemicals, chromatographic separations were performed as described for characterization analysis. Triple quadrupole scans were acquired in MRM mode on an AB SCIEX QTRAP 5500 LC-MS/MS system, equipped with an electrospray ionization (ESI) Turbo Ion-Spray interface, operating in the negative ionization mode and controlled by Analyst 1.6 software (AB SCIEX, Framingham, MA). The ESI source operation parameters were as follows: source temperature, 550 °C; ion-spray voltage, −4.5 kV; and ion source gas I, gas II, and curtain gas, 55, 55, and 35 psi, respectively. Optimization of MS parameters for each selected mass transition was carried out through direct infusion of a mixed standard solution. The peak areas of all analytes were acquired in MRM mode for quantification. Calibration curves were determined experimentally for available standards. Because of the lack of standards for some tentatively identified compounds, their Q1 and Q3 were set as quasi-molecular ions and the most abundant MS/MS fragment, respectively, the DP values were optimized at −80, −120, and −150 V, and the CE values were optimized at −20, −35, and −50 eV. Their calibration curves were determined with some other available standards. Among phenolic acid and derivatives, ellagic acid derivatives were relatively quantified based on ellagic acid content and others were relatively quantified according to the content of *p*-coumaric acid. Flavonoids and derivatives were relatively quantified based on the isoquercetrin content, except for myricitrin. Among proanthocyanidins and derivatives, EGCG−EGCG was relatively quantified based on the EGCG content, and others were relatively quantified based on the (E)GC content. All determinations were performed in triplicate. MultiQuant version 3.0.2 (AB SCIEX, Framingham, MA) was used for data processing.

Animals and Diets. Male KK-A^y mice of 5 week age were bought from Beijing HFK Bioscience Co., Ltd. (Beijing, China) and kept in a special facility without specific pathogens. Each cage housed three or four mice under 12 h light/dark cycles. During the overall experiment, mice were fed water and a diabetic diet (1K65, Beijing HFK Bioscience Co., Ltd., Beijing, China) ad libitum. Diet composition was as follows:[21] protein 180 g/kg; water, 80 g/kg; crude ash, 70 g/kg; fat, 60 g/

https://dx.doi.org/10.1021/acsomega.0c02759
ACS Omega 2020, 5, 17839−17849

kg; crude fiber, 50 g/kg; P, 12 g/kg; Ca, 11 g/kg; K, 5 g/kg; Mg, 2 g/kg; Na, 2 g/kg; Cu, 10 mg/kg; Fe, 100 mg/kg; I, 0.5 mg/kg; Mn, 75 mg/kg; Se, 0.1 mg/kg; Zn, 30 mg/kg. After adaptation for 2 weeks, mice were randomly separated into two groups (n = 10). One was supplemented with the SJE dissolved in distilled water by gavage and the other was given water as a control, once a day for 5 weeks. The dosage of the SJE was 200 mg per kg BW, which was mainly based on a preliminary *in vivo* experiment. In addition, a group of C57BL/6 mice (n = 10) was chosen as a nondiabetic control.

Measurement of food intake and BW started from the first week and continued weekly for each mouse during the whole study. At the end of the experiment, mice were sacrificed by decapitation after diets withdrawn for 12 h and blood samples were immediately collected. Perirenal and epididymal WAT, and BAT, as well as the liver, kidneys, and the heart were weighed, frozen in liquid nitrogen instantly and stored at −80 °C until use. The tissue index (%) was calculated as follows: tissue weight (g)/BW (g) × 100. Such animal procedures were established according to the National Institutes of Health Guide for Care and Use of Laboratory and approved by the Committee on the Ethics of Animal Experiments of Zhejiang University. Our experiment's ethics approval code is ZJU20160443. Animal experiments were performed in compliance with all regulatory institutional guidelines for animal welfare (National Institutes of Health Publications, NIH Publications No. 80-23).

FBG, OGTT, and ITT. The FBG level was measured weekly using a One-Touch Ultra ZSJ 843ETT Glucometer (Johnson & Johnson). The OGTT and the ITT were performed during week 4 and week 5, respectively. All mice were fasted for 6 h before tests and then supplemented with water or the SJE by gavage. Mice were gavage with 2 g/kg BW glucose for the OGTT or injected with 1 IU/kg BW insulin for the ITT. Basal blood glucose levels were measured before oral glucose administration or insulin injection (0 min) by collection of blood samples from the tail vein. Later, additional blood glucose levels were detected every 30 min for 2 h in total.

Serum and Liver Analysis. Serum TG, TC, HDL-c, LDL-c, ALT, and aspartate transaminase (AST) were measured by a Cobas 8000 modular analyzer series (Roche, Switzerland). Serum adiponectin, resistin, leptin, glucagon, and insulin levels were detected by immunoassay using an ELISA kit (Shanghai Lengton Biological Technology Co., Ltd., Shanghai, China).

Hepatic TG and TC were analyzed by kits (Nanjing Jiancheng Bioengineering Institute, Nanjing, China) according to the manufacturer's instructions. Liver samples for histological analysis were fixed with 4% of paraformaldehyde/phosphate-buffered saline (PBS) (v/v), embedded in paraffin, and then stained with H&E or Oil red O. The stained section was visualized under a microscope (Olympus DP20, Japan) through the DP2-BSW image analysis software system with a magnification of 200×.

Quantitative Real-Time PCR. Total RNA from mice liver was extracted with Trizol reagent (Invitrogen) according to the manufacturer's protocols. In total RNA, trace contaminating genomic DNA was removed with TURBO DNase (Ambion, Austin). cDNA synthesis was started from 1 μg DNA-free RNA using the iScriptTM cDNA Synthesis Kit (Bio-Rad, Hercules, CA). Real-time PCR was conducted using a LightCycler480 real-time system (Roche, Switzerland). The reaction mixture (20 μL) consisted of 10 μL of SYBR Green Master I kit (Roche, Switzerland), 5 μL of cDNA, 1 μL of forward primer (10 μmol/L), and 1 μL of reverse primer (10 μmol/L). The housekeeping gene, *i.e.*, β-actin, was used as internal control. The primers used in this study are given in Table 3. Values of C_t were normalized to β-actin, and the $2^{-\Delta\Delta C_t}$ method was used to calculate the relative gene expression. The fold change of the SJE-supplemented group *vs* control group was determined to evaluate the treatment effect of the SJE on the relative gene expression level for every target gene.

Western Blot Analysis. Liver samples were lysed in RIPA buffer on ice for 5 min and then centrifuged at 4 °C, 12 000g for 15 min to obtain a protein-containing supernatant. The protein concentration was measured by the BCA method. Each protein (60 μg) was denatured and separated by a 10% sodium dodecyl sulfate (SDS)-polyacrylamide gel and then transferred onto a PVDF membrane (0.45 μm). Abundance of protein was detected with antibodies against phosphor-AMPKα (Thr172), AMPKα, and β-actin (1:1000 dilutions for each) and then incubated with peroxide-conjugated anti-rabbit immunoglobulin. Proteins were visualized by ECL (Pierce) and exposed by an X-ray film (Kodak). Each protein was normalized by β-actin, and normalization of specific protein phosphorylation was based on the corresponding protein.

Statistical Analysis. All data were analyzed using SPSS 19.0 statistical software (IBM, Armonk, NY) and expressed as mean ± standard error (SE). Differences shown in figures and tables were the comparison of the SJE-treated group and the KK-A^y control group treated with water by Student's t-test. The level at $p < 0.05$ was considered as a significant difference.

■ ASSOCIATED CONTENT

Supporting Information

The Supporting Information is available free of charge at https://pubs.acs.org/doi/10.1021/acsomega.0c02759.

Polyphenols at relatively lower levels identified by liquid chromatography quadrupole time-of-flight tandem mass spectrometry (LC-Q-TOF-MS) in the "Shui Jing" fruit extract (SJE) (Table S1) (PDF)

■ AUTHOR INFORMATION

Corresponding Author

Xian Li − *Zhejiang Provincial Key Laboratory of Horticultural Plant Integrative Biology/The State Agriculture Ministry Laboratory of Horticultural Plant Growth, Development and Quality Improvement, Zhejiang University, Hangzhou 310058, China*; orcid.org/0000-0002-9526-9031; Phone: (+86)-571-8898-1263; Email: xianli@zju.edu.cn; Fax: (+86)-571-8898-2224

Authors

Yilong Liu − *Zhejiang Provincial Key Laboratory of Horticultural Plant Integrative Biology/The State Agriculture Ministry Laboratory of Horticultural Plant Growth, Development and Quality Improvement, Zhejiang University, Hangzhou 310058, China*

Xianan Zhang − *Forestry and Fruit Research Institute, Shanghai Academy of Agricultural Sciences, Shanghai 201403, China*

Liuhuan Zhan − *Zhejiang Provincial Key Laboratory of Horticultural Plant Integrative Biology/The State Agriculture Ministry Laboratory of Horticultural Plant Growth, Development and Quality Improvement, Zhejiang University, Hangzhou 310058, China*

Chang Xu − *Zhejiang Provincial Key Laboratory of Horticultural Plant Integrative Biology/The State Agriculture Ministry Laboratory of Horticultural Plant Growth, Development and Quality Improvement, Zhejiang University, Hangzhou 310058, China*

Linxiao Sun − *Key Laboratory of Diagnosis and Treatment of Severe Hepato-Pancreatic Diseases of Zhejiang Province, Zhejiang Provincial Top Key Discipline in Surgery, Wenzhou Medical University First Affiliated Hospital, Wenzhou 325000, China;* orcid.org/0000-0001-5849-4881

Huamin Jiang − *Hangzhou Lichuan Ecological Agriculture Development Co., Ltd., Hangzhou 311123, China*

Chongde Sun − *Zhejiang Provincial Key Laboratory of Horticultural Plant Integrative Biology/The State Agriculture Ministry Laboratory of Horticultural Plant Growth, Development and Quality Improvement, Zhejiang University, Hangzhou 310058, China;* orcid.org/0000-0002-2874-0292

Complete contact information is available at: https://pubs.acs.org/10.1021/acsomega.0c02759

Author Contributions

[⊥]Y.L. and X.Z. contributed equally to this work.

Notes

The authors declare no competing financial interest.

■ ACKNOWLEDGMENTS

This work was supported by the National Key R&D Program of China (No. 2017YFE0102200), the National Natural Science Foundation of China (31872067), the 111 Project (B17039), and the Fundamental Research Funds for the Central Universities.

■ ABBREVIATIONS USED

SJE, "Shui Jing" fruit extract; EGCG, epigallocatechin gallate; T1D, type-1 diabetes; T2D, type-2 diabetes; IR, insulin resistance; C3G, cyanidin-3-*O*-glucoside; STZ, streptozotocin; LC-Q-TOF-MS, liquid chromatography quadrupole time-of-flight mass spectrometry; MRM, multiple reaction monitoring; BW, bodyweight; WAT, white adipose tissue; BAT, brown adipose tissue; FBG, fasting blood glucose; OGTT, oral glucose tolerance test; ITT, insulin tolerance test; TG, triglyceride; TC, total cholesterol; HDL-c, high-density lipoprotein cholesterol; LDL-c, low-density lipoprotein cholesterol; ALT, alanine aminotransferase; AST, aspartate transaminase; PAs, proanthocyanidins; RA, relative abundance; RT, retention time

■ REFERENCES

(1) American Diabetes Association. Classification and diagnosis of diabetes: standards of medical care in diabetes-2018. *Diabetes Care* **2018**, *41*, S13−S27.

(2) *Global Report on Diabetes*; World Health Organization: Geneva, 2016.

(3) Cho, N. H.; Shaw, J. E.; Karuranga, S.; Huang, Y.; da Rocha Fernandes, J. D.; Ohlrogge, A. W.; Malanda, B. IDF diabetes atlas: global estimates of diabetes prevalence for 2017 and projections for 2045. *Diabetes Res. Clin. Pract.* **2018**, *138*, 271−281.

(4) Wong, E.; Backholer, K.; Gearon, E.; Harding, J.; Freak-Poli, R.; Stevenson, C.; Peeters, A. Diabetes and risk of physical disability in adults: a systematic review and meta-analysis. *Lancet Diabetes Endocrinol.* **2013**, *1*, 106−114.

(5) Muraki, I.; Imamura, F.; Manson, J. E.; Hu, F. B.; Willett, W. C.; van Dam, R. M.; Sun, Q. Fruit consumption and risk of type 2 diabetes: results from three prospective longitudinal cohort studies. *BMJ* **2013**, *347*, No. f5001.

(6) Li, S.; Miao, S.; Huang, Y.; Liu, Z.; Tian, H.; Yin, X.; Tang, W.; Steffen, L. M.; Xi, B. Fruit intake decreases risk of incident type 2 diabetes: an updated meta-analysis. *Endocrine* **2015**, *48*, 454−460.

(7) Vendrame, S.; Del Bo', C.; Ciappellano, S.; Riso, P.; Klimis-Zacas, D. Berry Fruit Consumption and Metabolic Syndrome. *Antioxidants* **2016**, *5*, No. 34.

(8) Castro-Acosta, M. L.; Lenihan-Geels, G. N.; Corpe, C. P.; Hall, W. L. Berries and anthocyanins: promising functional food ingredients with postprandial glycaemia-lowering effects. *Proc. Nutr. Soc.* **2016**, *75*, 342−355.

(9) Liu, W.; Mao, Y.; Schoenborn, J.; Wang, Z.; Tang, G.; Tang, X. Whole blueberry protects pancreatic beta-cells in diet-induced obese mouse. *Nutr. Metab.* **2019**, *16*, No. 34.

(10) Rocha, D. M. U. P.; Caldas, A. P. S.; da Silva, B. P.; Hermsdorff, H. H. M.; Alfenas, R. D. C. G. Effects of blueberry and cranberry consumption on type 2 diabetes glycemic control: a systematic review. *Crit. Rev. Food Sci. Nutr.* **2019**, *59*, 1816−1828.

(11) Yan, F.; Zhang, J.; Zhang, L.; Zheng, X. Mulberry anthocyanin extract regulates glucose metabolism by promotion of glycogen synthesis and reduction of gluconeogenesis in human HepG2 cells. *Food Funct.* **2016**, *7*, 425−433.

(12) Yan, F.; Dai, G.; Zheng, X. Mulberry anthocyanin extract ameliorates insulin resistance by regulating PI3K/AKT pathway in HepG2 cells and db/db mice. *J. Nutr. Biochem.* **2016**, *36*, 68−80.

(13) Spínola, V.; Pinto, J.; Llorent-Martínez, E. J.; Tomás, H.; Castilho, P. C. Evaluation of *Rubus grandifolius* L. (wild blackberries) activities targeting management of type-2 diabetes and obesity using in vitro models. *Food Chem. Toxicol.* **2019**, *123*, 443−452.

(14) Bispo, K.; Amusquivar, E.; García-Seco, D.; Ramos-Solano, B.; Gutierrez-Mañero, J.; Herrera, E. Supplementing diet with blackberry extract causes a catabolic response with increments in insulin sensitivity in rats. *Plant Foods Hum. Nutr.* **2015**, *70*, 170−175.

(15) Bao, J.; Cai, Y.; Sun, M.; Wang, G.; Corke, H. Anthocyanins, flavonols, and free radical scavenging activity of Chinese bayberry (*Myrica rubra*) extracts and their color properties and stability. *J. Agric. Food Chem.* **2005**, *53*, 2327−2332.

(16) Zhang, X.; Huang, H.; Zhang, Q.; Fan, F.; Xu, C.; Sun, C.; Li, X.; Chen, K. Phytochemical characterization of Chinese bayberry (*Myrica rubra* Sieb. et Zucc.) of 17 cultivars and their antioxidant properties. *Int. J. Mol. Sci.* **2015**, *16*, 12467−12481.

(17) Zhang, X.; Huang, H.; Zhao, X.; Lv, Q.; Sun, C.; Li, X.; Chen, K. Effects of flavonoids-rich chinese bayberry (*Myrica rubra* sieb. et zucc.) pulp extracts on glucose consumption in human HepG2 cells. *J. Funct. Foods* **2015**, *14*, 144−153.

(18) Cai, H.; Yang, B.; Xu, Z.; Zhang, B.; Xu, B. Y.; Li, X.; Wu, P.; Chen, K. S.; Rajotte, R. V.; Wu, Y. L.; Rayat, G. R. Cyanidin-3-O-glucoside enhanced the function of syngeneic mouse islets transplanted under the kidney capsule or into the portal vein. *Transplantation* **2015**, *99*, 508−514.

(19) Li, C.; Yang, B.; Xu, Z.; Boivin, E.; Black, M.; Huang, W. L.; Xu, B. Y.; Wu, P.; Zhang, B.; Li, X.; Chen, K. S.; Wu, Y. L.; Raya, G. R. Protective effect of cyanidin-3-O-glucoside on neonatal porcine islets. *J. Endocrinol.* **2017**, *235*, 237−249.

(20) Sun, C. D.; Zhang, B.; Zhang, J. K.; Xu, C. J.; Wu, Y. L.; Li, X.; Chen, K. S. Cyanidin-3-glucoside-rich extract from Chinese bayberry fruit protects pancreatic β cells and ameliorates hyperglycemia in streptozotocin-induced diabetic mice. *J. Med. Food* **2012**, *15*, 288−298.

(21) Zhang, X.; Lv, Q.; Jia, S.; Chen, Y. H.; Sun, C. D.; Li, X.; Chen, K. S. Effects of flavonoid-rich Chinese bayberry (*Morella rubra* Sieb. et Zucc.) fruit extract on regulating glucose and lipid metabolism in diabetic KK-Ay mice. *Food Funct.* **2016**, *7*, 3130−3140.

(22) Lee, R. J.; Lee, V. S.; Tzen, J. T.; Lee, M. R. Study of the release of gallic acid from (-)-epigallocatechin gallate in old oolong tea by

mass spectrometry. *Rapid Commun. Mass Spectrom.* **2010**, *24*, 851−858.
(23) Schmidt, C. A.; Murillo, R.; Heinzmann, B.; Laufer, S.; Wray, V.; Merfort, I. Structural and conformational analysis of proanthocyanidins from Parapiptadenia rigida and their wound-healing properties. *J. Nat. Prod.* **2011**, *74*, 1427−1436.
(24) Zhou, J.; Wu, Y.; Long, P.; Ho, C. T.; Wang, Y. J.; Kan, Z. P.; Cao, L. T.; Zhang, L.; Wan, X. C. LC-MS-Based Metabolomics reveals the chemical changes of polyphenols during high-temperature roasting of large-leaf yellow tea. *J. Agric. Food Chem.* **2019**, *67*, 5405−5412.
(25) Olennikov, D. N.; Kashchenko, N. I.; Akobirshoeva, A. Phenolic compounds and hydroxynitrile glycosides from roots of *Rhodiola recticaulis* and *R. gelida*. *Chem. Nat. Compd.* **2019**, *55*, 948−950.
(26) Xie, L. F.; Cao, Y. L.; Zhao, Z. K.; Ren, C. H.; Xing, M. Y.; Wu, B. P.; Zhang, B.; Xu, C. J.; Chen, K. S.; Li, X. Involvement of MdUGT75B1 and MdUGT71B1 in flavonol galactoside/glucoside biosynthesis in apple fruit. *Food Chem.* **2020**, *312*, No. 126124.
(27) Ruslay, S.; Abas, F.; Shaari, K.; Zainal, Z.; Maulidiani; Sirat, H.; Israf, D. A.; Lajis, N. H. Characterization of the components present in the active fractions of health gingers (*Curcuma xanthorrhiza* and *Zingiber zerumbet*) by HPLC-DAD-ESIMS. *Food Chem.* **2007**, *104*, 1183−1191.
(28) Rodrigues, C. M.; Rinaldo, D.; Sannomiya, M.; Santos, L. C.; Montoro, P.; Piacente, S.; Pizza, C.; Vilegas, W. High-performance liquid chromatographic separation and identification of polyphenolic compounds from the infusion of *Davilla elliptica* St. Hill. *Phytochem. Anal.* **2008**, *19*, 17−24.
(29) Pfundstein, B.; El Desouky, S. K.; Hull, W. E.; Haubner, R.; Erben, G.; Owen, R. W. Polyphenolic compounds in the fruits of Egyptian medicinal plants (*Terminalia bellerica*, *Terminalia chebula* and *Terminalia horrida*): characterization, quantitation and determination of antioxidant capacities. *Phytochemistry* **2010**, *71*, 1132−1148.
(30) Koss-Mikołajczyk, I.; Kusznierewicz, B.; Bartoszek, A. The relationship between phytochemical composition and biological activities of differently pigmented varieties of berry fruits; comparison between embedded in food matrix and isolated anthocyanins. *Foods* **2019**, *8*, No. 646.
(31) Srikanta, A. H.; Kumar, A.; Sukhdeo, S. V.; Peddha, M. S.; Govindaswamy, V. The antioxidant effect of mulberry and jamun fruit wines by ameliorating oxidative stress in streptozotocin-induced diabetic Wistar rats. *Food Funct.* **2016**, *7*, 4422−4431.
(32) Chakrawarti, L.; Agrawal, R.; Dang, S.; Gupta, S.; Gabrani, R. Therapeutic effects of EGCG: a patent review. *Expert Opin. Ther. Pat.* **2016**, *26*, 907−916.
(33) Kapoor, M. P.; Sugita, M.; Fukuzawa, Y.; Okubo, T. Physiological effects of epigallocatechin-3-gallate (EGCG) on energy expenditure for prospective fat oxidation in humans: a systematic review and meta-analysis. *J. Nutr. Biochem.* **2017**, *43*, 1−10.
(34) Straub, L. G.; Efthymiou, V.; Grandl, G.; Balaz, M.; Challa, T. D.; Truscello, L.; Horvath, C.; Moser, C.; Rachamin, Y.; Arnold, M.; Sun, W.; Modica, S.; Wolfrum, C. Antioxidants protect against diabetes by improving glucose homeostasis in mouse models of inducible insulin resistance and obesity. *Diabetologia* **2019**, *62*, 2094−2105.
(35) Dembinska-Kiec, A.; Mykkanen, O.; Kiec-Wilk, B.; Mykkanen, H. Antioxidant phytochemicals against type 2 diabetes. *Br. J. Nutr.* **2008**, *99*, ES109−ES117.
(36) Lv, Q.; Si, M.; Yan, Y.; Luo, F.; Hu, G.; Wu, H.; Sun, C. D.; Li, X.; Chen, K. S. Effects of phenolic-rich litchi (*Litchi chinensis* Sonn.) pulp extracts on glucose consumption in human HepG2 cells. *J. Funct. Foods* **2014**, *7*, 621−629.
(37) Lv, Q.; Luo, F.; Zhao, X.; Liu, Y.; Hu, G. B.; Sun, C. D.; Li, X.; Chen, K. S. Identification of proanthocyanidins from litchi (*Litchi chinensis* Sonn.) pulp by LC-ESI-Q-TOF-MS and their antioxidant activity. *PLoS One* **2015**, *10*, No. e0120480.
(38) Jia, Y.; Ma, Y.; Cheng, G.; Zhang, Y.; Cai, S. Comparative study of dietary flavonoids with different structures as α-glucosidase inhibitors and insulin sensitizers. *J. Agric. Food Chem.* **2019**, *67*, 10521−10533.
(39) Ahangarpour, A.; Oroojan, A. A.; Khorsandi, L.; Kouchak, M.; Badavi, M. Antioxidant effect of myricitrin on hyperglycemia-induced oxidative stress in C2C12 cell. *Cell Stress Chaperones* **2018**, *23*, 773−781.
(40) Ahangarpour, A.; Oroojan, A. A.; Khorsandi, L.; Kouchak, M.; Badavi, M. Solid Lipid nanoparticles of myricitrin have antioxidant and antidiabetic effects on streptozotocin-nicotinamide-induced diabetic model and myotube cell of male mouse. *Oxid. Med. Cell. Longevity* **2018**, *2018*, No. 7496936.
(41) Saltiel, A. R.; Kahn, C. R. Insulin signalling and the regulation of glucose and lipid metabolism. *Nature* **2001**, *414*, 799−806.
(42) Frühbeck, G.; Salvador, J. Relation between leptin and the regulation of glucose metabolism. *Diabetologia* **2000**, *43*, 3−12.
(43) Quesada, I.; Tudurí, E.; Ripoll, C.; Nadal, A. Physiology of the pancreatic alpha-cell and glucagon secretion: role in glucose homeostasis and diabetes. *J. Endocrinol.* **2008**, *199*, 5−19.
(44) Godoy-Matos, A. F. The role of glucagon on type 2 diabetes at a glance. *Diabetol. Metab. Syndr.* **2014**, *6*, No. 91.
(45) DeFronzo, R. A.; Ferrannini, E.; Simonson, D. C. Fasting hyperglycemia in non-insulin-dependent diabetes mellitus: contributions of excessive hepatic glucose production and impaired tissue glucose uptake. *Metabolism* **1989**, *38*, 387−395.
(46) Koo, S. H.; Flechner, L.; Qi, L.; Zhang, X. M.; Screaton, R. A.; Jeffries, S.; Hedrick, S.; Xu, W.; Boussouar, F.; Brindle, P.; Takemori, H.; Montminy, M. The CREB coactivator TORC2 is a key regulator of fasting glucose metabolism. *Nature* **2005**, *437*, 1109−1111.
(47) Zhang, Y.; Huang, N. Q.; Yan, F.; Jin, H.; Zhou, S. Y.; Shi, S. J.; Jin, F. Diabetes mellitus and Alzheimer's disease: GSK-3β as a potential link. *Behav. Brain Res.* **2018**, *339*, 57−65.
(48) Tanabe, K.; Liu, Z.; Patel, S.; Doble, B. W.; Li, L.; Cras-Méneur, C.; Martinez, S. C.; Welling, C. M.; White, M. F.; Bernal-Mizrachi, E.; Woodgett, J. R.; Permutt, M. A. Genetic deficiency of glycogen synthase kinase-3beta corrects diabetes in mouse models of insulin resistance. *PLoS Biol.* **2008**, *6*, No. e37.
(49) Kim, J. J.; Tan, Y.; Xiao, L.; Sun, Y. L.; Qu, X. Green tea polyphenol epigallocatechin-3-gallate enhance glycogen synthesis and inhibit lipogenesis in hepatocytes. *Biomed. Res. Int.* **2013**, *2013*, No. 920128.
(50) Vinayagam, R.; Jayachandran, M.; Xu, B. Antidiabetic effects of simple phenolic acids: a comprehensive review. *Phytother. Res.* **2016**, *30*, 184−199.
(51) Cheng, A.; Saltiel, A. R. More TORC for the gluconeogenic engine. *BioEssays* **2006**, *28*, 231−234.
(52) Zhang, B. B.; Zhou, G.; Li, C. AMPK: an emerging drug target for diabetes and the metabolic syndrome. *Cell Metab.* **2009**, *9*, 407−416.
(53) Radziuk, J.; Bailey, C. J.; Wiernsperger, N. F.; Yudkin, J. S. Metformin and its liver targets in the treatment of type 2 diabetes. *Curr. Drug Targets: Immune, Endocr. Metab. Disord.* **2003**, *3*, 151−169.
(54) Caton, P. W.; Nayuni, N. K.; Kieswich, J.; Khan, N. Q.; Yaqoob, M. M.; Corder, R. Metformin suppresses hepatic gluconeogenesis through induction of SIRT1 and GCN5. *J. Endocrinol.* **2010**, *205*, 97−106.
(55) Laplante, M.; Sabatini, D. M. mTOR signaling at a glance. *J. Cell Sci.* **2009**, *122*, 3589−3594.
(56) Shaw, R. J. LKB1 and AMP-activated protein kinase control of mTOR signalling and growth. *Acta Physiol.* **2009**, *196*, 65−80.
(57) Hay, N.; Sonenberg, N. Upstream and downstream of mTOR. *Genes Dev.* **2004**, *18*, 1926−1945.
(58) Navarro, I.; Leibush, B.; Moon, T. W.; Plisetskaya, E. M.; Baños, N.; Méndez, E.; Planas, J. V.; Gutiérrez, J. Insulin, insulin-like growth factor-I (IGF-I) and glucagon: the evolution of their receptors. *Comp. Biochem. Physiol., Part B: Biochem. Mol. Biol.* **1999**, *122*, 137−153.
(59) Tseng, Y. T.; Hsu, H. T.; Lee, T. Y.; Chang, W. H.; Lo, Y. C. Naringenin, a dietary flavanone, enhances insulin-like growth factor 1 receptor-mediated antioxidant defense and attenuates methylglyoxal-

https://dx.doi.org/10.1021/acsomega.0c02759
ACS Omega 2020, 5, 17839−17849

induced neurite damage and apoptotic death. *Nutr. Neurosci.* **2019**, 1−11.
(60) Christiaens, V.; Van Hul, M.; Lijnen, H. R.; Scroyen, I. CD36 promotes adipocyte differentiation and adipogenesis. *Biochim. Biophys. Acta* **2012**, *1820*, 949−956.
(61) Wang, D.; Xia, M.; Gao, S.; Li, D.; Zhang, Y.; Jin, T.; Ling, W. H. Cyanidin-3-O-β-glucoside upregulates hepatic cholesterol 7α-hydroxylase expression and reduces hypercholesterolemia in mice. *Mol. Nutr. Food Res.* **2012**, *56*, 610−621.
(62) Othman, A. I.; El-Sawi, M. R.; El-Missiry, M. A.; Abukhalil, M. H. Epigallocatechin-3-gallate protects against diabetic cardiomyopathy through modulating the cardiometabolic risk factors, oxidative stress, inflammation, cell death and fibrosis in streptozotocin-nicotinamide-induced diabetic rats. *Biomed. Pharmacother.* **2017**, *94*, 362−373.

https://dx.doi.org/10.1021/acsomega.0c02759
ACS Omega 2020, 5, 17839−17849